# NRC Publications Archive (NPArC)
# Archives des publications du CNRC (NPArC)

## Cracking and Spalling Behavior of WC-17% Co Cermet Coatings

Legoux, Jean-Gabriel; Bouaricha, Salim; Sauer, John P.

**Web page / page Web**

http://nparc.cisti-icist.nrc-cnrc.gc.ca/npsi/ctrl?action=rtdoc&an=15877985&lang=en
http://nparc.cisti-icist.nrc-cnrc.gc.ca/npsi/ctrl?action=rtdoc&an=15877985&lang=fr

National Research Council Canada    Conseil national de recherches Canada

Canada

# Cracking and Spalling Behavior of WC-17% Co Cermet Coatings.

*Jean-Gabriel Legoux, Salim Bouaricha*
*Industrial Materials Institute, National Research Council Canada, Boucherville, Québec, Canada*
*John P. Sauer*
*Sauer Engineering, Cincinnati, OH, USA*

## Abstract

Thermal spray WC based powders are now frequently used as chrome replacement alternatives for a wide range of industrial and aeronautical applications. In numerous cases, the carbide materials outperform the hard chrome in many property evaluations. However, their usage on highly stressed parts, especially in fatigue loading, can be limited by spalling resistance of the coating. While HVOF is being used on many flight critical parts, stringent applications like the landing gear components of carrier-based aircraft are still under investigation.

This work, on WC-17%Co, relates coating bend test performance and fatigue/cyclic step loading behavior to the processing history using different HVOF systems. Initially, twelve (12) different coatings were monitored using a DPV-2000 for temperature/velocity profiles. The mechanical properties were then assessed using an instrumented four-point bend test as well as uniaxial cyclic loading.

After mechanical testing, the coating microstructures were characterized using X-Ray diffraction and electron microscopy in order to investigate the phase content and nature. In particular, the cracks generated during the bend test were measured using SEM on sample cross sections to understand characteristics such as spacing and crack penetration to the substrate. The interactions of processing parameters with the cracking/spalling resistance of the various coating deposits will be discussed and a potential criteria for the control of cracking phenomena will be presented.

## Introduction

The HCAT and C-HCAT programs have been very successful in demonstrating the possibility of replacing hard chrome plating on aeronautical parts, particularly on landing gears. The results obtained to date show that the fatigue debit associated with the HVOF coating is small as compared to that of hard chrome, and that both the corrosion properties can be very good and wear resistance is improved. Commercial and military flight tests are ongoing and the testing of components has also been performed in the C-HCAT program. One of the experimental problems that was raised by the test programs comes from an indication that, for parts submitted to high strain, both the WC-17%Co coatings and WC-10%Co-4%Cr coatings have a tendency to spall. However, even if most of the parts to be coated will never be subjected to stresses near or over their elastic limit (high strain), some critical applications may require the best possible strain resistance.

The experimental efforts generated for the HCAT/C-HCAT programs were extensive: coatings with different chemistries were sprayed using varied guns or gases and tested in different regimes on numerous substrates. Also, the evaluations were conducted at a variety of different spray sources and laboratories. Since all the experiments were not performed with the same objective, coating characterization was not uniform. With many variations, it is therefore very difficult to compare and understand the spalling behavior of coatings. This work was undertake to address the variation in spray parameters/location and the lack of a uniform testing objective.

## Experimentals

### Materials

The powders recommended by the manufacturer were used with each gun. A single powder lot from the manufacturer was used: the Diamalloy 2005 for the Diamond Jet (Sulzer, Westburry, NY), the Stelcar JK 117 for the Jet Kote (Stellite Coatings, Goshen, IN) and the 1343 VM for the JP-5000 (TAFA, Concord., NH). The powders are presented in Fig. 1. The three powders are similar; however, upon cross section, the D-2005NS shows more porosity than the other powders and seems to be constituted of discrete/fine particles possibly because of less sintering after the agglomeration.
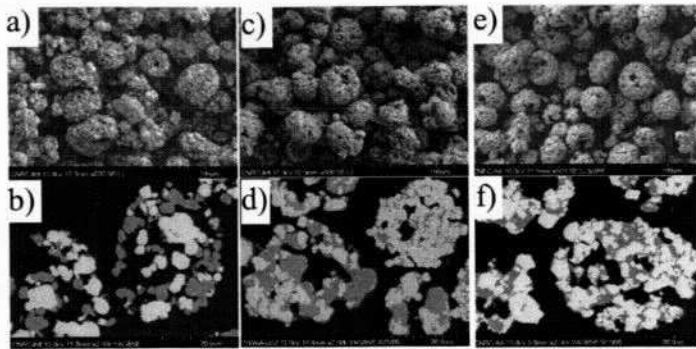
*Figure 1  Appearance and cross section of powders a) and b) Diamalloy 2005 NS  c) and d) 1343 VM, e) and f) JK-117*

## Thermal Spraying and Particles In-Flight properties

Conditions were selected based on past HCAT experiments in order to cover the operational ranges for each system. The in-flight temperature and velocity were measured during spraying using a DPV-2000 system (Tecnar Automation, St.-Bruno, Québec, Canada). Table 1 lists these data.

***Table 1:*** *Sets of thermal spray parameters used for the HVOF guns to produce samples and in-flight particles temperature and velocity obtained by DPV-2000..*

| Sample ID | $O_2$ flow | $H_2$ flow | Air flow | Carrier | Powder feed | SOD | Temp | Velocity |
|---|---|---|---|---|---|---|---|---|
| | (lpm) | (lpm) | (lpm) | (lpm) | (g/min) | (in.) | (°C) | (m/s) |
| DJ2 | 225 | 717 | 322 | 17.5 | 38 | 21.6 | 2025 | 668 |
| DJ4 | 231 | 684 | 371 | 17.5 | 38 | 21.6 | 2002 | 680 |
| DJ5 | 196 | 581 | 413 | 17.5 | 38 | 29.2 | 1846 | 589 |
| DJ6 | 180 | 706 | 405 | 17.5 | 38 | 29.2 | 1857 | 680 |
| | $O_2$ flow | $H_2$ flow | Nozzle | Carrier | Powder feed | SOD | Temp | Velocity |
| | (lpm) | (lpm) | (cm) | (lpm) | (g/min) | (in.) | (°C) | (m/s) |
| JK2 | 269 | 543 | 22.9 | 27 | 54.6 | 17.8 | 1853 | 592 |
| JK4 | 330 | 661 | 22.9 | 27 | 51.6 | 17.8 | 1920 | 620 |
| JK5 | 330 | 661 | 22.9 | 27 | 44 | 25.4 | 1770 | 560 |
| JK7 | 330 | 661 | 15.2 | 27 | 50.9 | 17.8 | 1918 | 566 |
| JK8 | 330 | 736 | 22.9 | 27 | 50 | 12.7 | 1875 | 622 |
| | K1 flow | $O_2$ flow | Barrel | Carrier | Powder feed | SOD | Temp | Velocity |
| | (lph) | (lpm) | (cm) | (lpm) | (g/min) | (in.) | (°C) | (m/s) |
| JP 1-3 | 23.5 | 967 | 10.2 | 11.8 | 80 | 38.1 | 1791 | 683 |
| JP 4-6 | 18.9 | 944 | 20.3 | 11.8 | 80 | 45.7 | 1608 | 592 |
| JP 7-9 | 18.9 | 944 | 15.2 | 11.8 | 80 | 40.6 | 1667 | 636 |
| JP10-12 | 22.7 | 932 | 15.2 | 11.8 | 80 | 35.6 | 1852 | 717 |

Four (4) sets of thermal spray conditions were selected for the Diamond Jet (DJ involving two (2) spray distances with constant carrier gas/feed rate combinations and subsequent variation of the primary gas flows.

For the Jet Kote (JK) system, five (5) sets of thermal spray conditions were selected to cover the operating range without further optimization.

Four conditions were selected to produce coatings using the JP-5000 (JP) involving 3 different barrel lengths.. These conditions involved the lowest temperature (1608 °C) and the highest velocities (717 m/s) of the three guns.

Figure 2 shows the resultant difference in temperature/velocity profiles between the three different spray systems illustrating

the design variation in combining kinetic/thermal energy to form the final coating deposit.
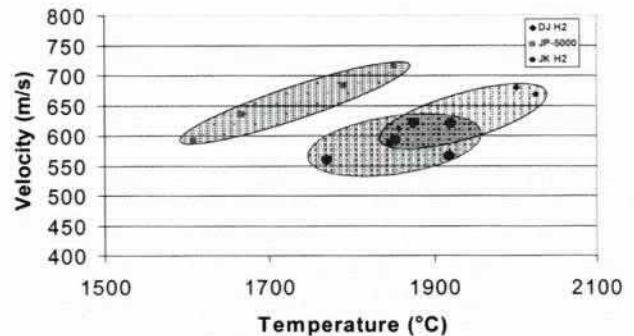


*Figure 2  Temperature/Velocity for the Varied HVOF Conditions  (Note this is the operating range for this study)*

## Sample Production

Coatings were produced on two type of samples, the Almen N strips were used to characterize the microstructure, residual stresses and the four point bending. The coating of Almen strips was performed on a 3.5 in. diameter cylinder to enable proper holding and cooling of the strips. Four strips were sprayed at the same time. For the step loading experiment and fatigue testing, coatings were produced on .250" diameter hour glass bars. The coatings were sprayed on shot peened 300M samples to a nominal thickness of 5 mils and were subsequently ground to 3 mils. Also, for one condition per gun, one set of four bars was sprayed to a larger thickness of 18 mils (15 mils after grinding). For both types of specimens, the temperature of the substrate was monitored using an optical infared (IR) pyrometer. The maximum surface temperature was kept at 200°C (400°F) because of the different spray distances and gas parameters while the minimum spray temperature for the substrate (between passes) varied from 85°C to 165 °C.

## Coating Characterization

*Residual stresses*

The residual stresses are reported as the average value of the four Almen N strips. Positive values indicate compressive residual stresses. Stresses have been normalized for a thickness of 125 µm (.005").

*X-Ray Diffraction (XRD)*

X-ray diffraction measurements were carried out using a Bruker-AXS diffractometer with Cu-$K_\alpha$ radiation to determine the phases present in the coatings. The X-ray diffraction patterns for all coatings were examined. The data shows that all coatings consist of WC as the major phase, with $W_2C$ and W in small amounts resulting from the WC decarburization.

No clear peak related to the Co phase was found. In addition, a broad diffraction halo at a range of $2\theta \approx (37°, 47°)$ is also present indicating the presence of a quantity of an amorphous or nanocrystalline phase in each coating, probably composed of W, Co and C. From the spectrum, it is possible to determine the index of crystallinity ($I_c$). The $I_c$ is defined as the ratio between the areas of the Bragg peaks (crystalline material) and the total areas of the spectrum for $2\theta$ comprised between 30 and 55 degrees. It is important to note that $I_c$ values are not absolute but can be used to rank the materials in a relative manner: a higher $I_c$ indicates the coating is composed of more crystalline material.

*Four-Point Bending Procedure*

For this work, the set-up already described in [1-2] was used. The lengths of the inner and outer spans were 20 mm and 50 mm, respectively.

Tensile bending tests were performed on all coatings. A maximum deflection of 5 mm was imposed on all samples and corresponds by calculation to about 0.91% strain for 1 mm thick sample in the tensile surface of the substrate. The value of 5 mm in deflection was chosen in such way that after loading the substrate alone (Almen strip without coating), no permanent bending was present.

*Acoustic Emission Testing Procedure*

Acoustic transducers were placed on samples during the bending in order to quantify the emissions produced during testing. The acoustic emission (AE) signals were detected by a piezoelectric sensor having a diameter of 6 mm (Panametrics, Mtl., Québec) and a frequency response up to 1.5 MHz. For the bend testing investigation, the onset of cracking, the number of events, the energy per events and the cumlative energy were measured and reported.

*Microstructure Characterization*

The coatings were examined using a Hitachi S-4700 scanning electron microscope (SEM). The average coating thickness for all coatings was estimated from SEM micrograph. The polished longitudinal side planes between the inner spans of the four-point bend test were observed. The preparation technique involved double vacuum infiltration and proper polishing in order to preserve the cracks generated during bending. The following data was gathered: **D**, the mean distance between two successive cracks **D$_{int}$** the distance of propagation at interface, from these values **I$_s$** the index of spalling defined as the ratio of "D$_{int}$/D" is computed (Fig. 3).

## Cyclic stress testing.

Two type of mechanical testing were performed using the hour glass type bars.
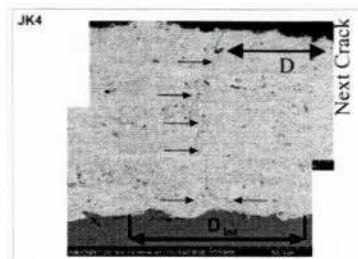


*Figure 3: Example of crack characterization on JK4 coating*

The Integrity testing was performed to evaluate the stress level at which stress cracking or spalling would occur when applied to the coated bars. All integrity and fatigue testing was performed using a R ratio of –0.5. Integrity tests were performed by axially loading samples at a stress level of 1241 MPa (180 ksi) for 100 cycles then increasing step loading at 69 MPa (10 ksi)/100 cycles increments until observation of cracking or any sign of spalling on the samples. Two (2) bars were used for this testing: for one of the bars, the test was interrupted when first indication of cracking was noticed. For the second bar, the cracked samples was then tested further to spalling.

Fatigue testing was performed at 1310 MPa(190 ksi) for all the spray conditions for the thin coatings and 1103 MPa (160 ksi) for the thick ones. After cracking was observed, one of the cracked samples was then  tested further to spalling or to sample faillure.

### Results and Discussion

None of the studied coatings spalled or delaminated from the substrates. All coatings exhibited clearly defined transverse cracks. The cracks apparently propagated from the surface normal to the load axis and into the coating-substrate interface without branches allowing for subsequent propagation parallel to and along the substrate interface. Similar behavior has been observed previously [1-4].  Results of coating evaluation are reported in Table 2.

Table 2 also shows the crystallinity index for all coatings. For example, the coatings made using the JP-5000 have a higher index of crystallinity. These coatings were also produced from particles having the lower temperature during their transit from the gun to the substrate as shown in Figure 2. Figure 4 shows the relationship between the index of crystallinity and processing temperature.  This illustrates how the in-flight temperature has a direct influence on the decarburization and solutionizing of the coating hard phase. Indeed, an increasing temperature leads to a decrease of the crystallinity for the coatings. This relationship appears to apply for the 3 systems.

An intuitive technical prejudice from an engineering standpoint that may be the possible effect of  residual stresses regarding coating spalliation.  It should be noted that the general trend is to observe a reduction of the "I$_s$", while the

residual stresses increase. Technical logic would seem to indciate a higher residual stress (compressive) in a coating would be manifested in a lower resulting strain (in tension) when an opposite stress is applied. However, it should also be noted that the correlation between the residual stress and the $I_s$ (Index of Spalling) is not good indicating that other factors are strongly influencing the spalling behavior of coatings.

*Table 2 Microstructural evaluation.*

| ID # | Thickness of coating* (μm) | Residual Stress*** (μm-mils) | H,**** (VHN 300 g) | D:* (mm) | D_hu: (μm) | $I_s$ | $I_c$:*** |
|---|---|---|---|---|---|---|---|
| DJ2 | 215 | 344 | 1186.1 | 1.090 | 355 | 0.326 | 0.406 |
| DJ4 | 190 | 476 | 1159.3 | 0.911 | 213 | 0.234 | 0.418 |
| DJ5 | 236 | 278 | 1169.9 | 1.573 | 1014 | 0.645 | 0.509 |
| DJ6 | 214 | 344 | 1194.1 | 1.326 | 621 | 0.468 | 0.512 |
| JK2 | 120 | 221 | 1166.5 | 0.585 | 195 | 0.333 | 0.565 |
| JK4 | 128 | 414 | 1252.1 | 0.532 | 92 | 0.173 | 0.484 |
| JK5 | 108 | 168 | 1222 | 0.619 | 127 | 0.205 | 0.546 |
| JK7 | 136 | 103 | 1264.9 | 0.659 | 214 | 0.325 | 0.517 |
| JK8 | 140 | 351 | 1183.2 | 0.609 | 340 | 0.558 | 0.540 |
| JP1 | 79 | 479 | --. | 1.792 | 74 | 0.041 | |
| JP2 | 127 | 475 | -- | 0.628 | 193 | 0.307 | |
| JP3 | 224 | 256 | 1218 | 1.229 | 342 | 0.278 | 0.653 |
| JP4 | 99 | 296 | -- | 0.83 | 28.6 | 0.034 | |
| JP5 | 130 | 235 | -- | 0.7 | 260 | 0.371 | |
| JP6 | 203 | 203 | 1103 | 1.401 | 738 | 0.527 | 0.695 |
| JP7 | 83.82 | 414 | -- | 0.727 | 161 | 0.221 | |
| JP8 | 134.9 | 353 | -- | 0.695 | 155 | 0.223 | |
| JP9 | 203.2 | 263 | 1161 | 1.002 | 980 | 0.978 | 0.689 |
| JP10 | 78.7 | 570 | -- | 0.49 | 26.6 | 0.054 | |
| JP11 | 138.2 | 433 | -- | 0.674 | 110 | 0.163 | |
| JP12 | 201.2 | 358 | 1286 | 0.744 | 176 | 0.237 | 0.628 |

\* Estimated from SEM images.
\*\* Normalized to 125μm (5 mils) coating thickness.
\*\*\* Measured from X-ray diffraction patterns.
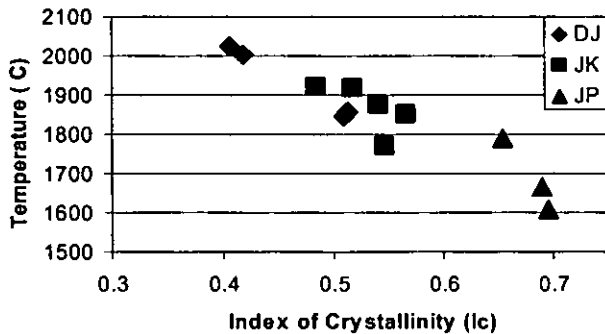\*\*\*\* an average of 10 readings



*Figure 4. In-Flight particle temperature vs. the index of crystallinity*

Figure 5 clearly shows that increasing coating thickness also increases the spalling tendency. Another technical prejudice from an engineering standpoint is an expectation that thicker coatings will show a higher tendency to spall; this is not the case for some points on the plot. Again, this indicates that spalling is not only affected by thickness but also by the varied spray conditions used during processing.

Microhardness is a quality control tool widely used in production. Figure 6 shows the relationship between microhardness and $I_c$. The data shows a good correlation within the systems but not for the combined information. This

could be related to use of different powders for each system. It would need to be studied in greater detail.
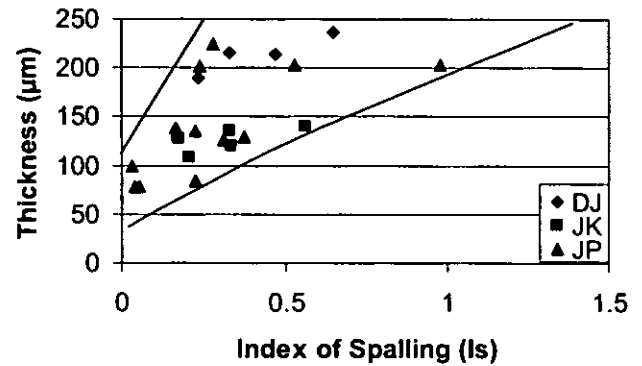


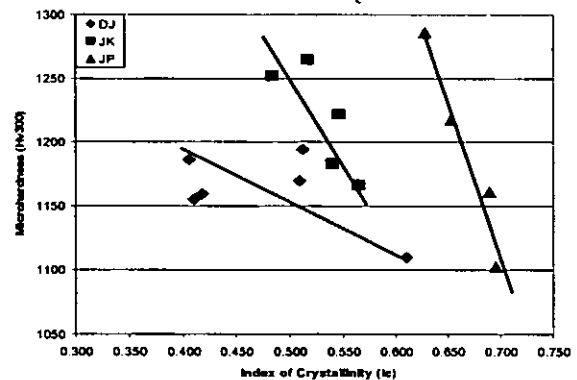*Figure 5  Relation between thickness of coatings and Index of Spalling ($I_s$).*



*Figure 6.  Microhardness vs. the index of crystallinity for coatings sprayed with the DJ, JK and JP systems.*

It is important to understand how coating structure ultimately affects the spalling tendency. Figure 7 shows that for each gun and varied thicknesses for the JP-5000, a direct relationship exists between $I_c$ and $I_s$. This indicates that a more crystalline coating has a larger tendency to spall. However, given the fact of the lines running parallel to each other, the trends for each system indicates the relationship is also intertwined with starting material and residual stress in the coating deposit.
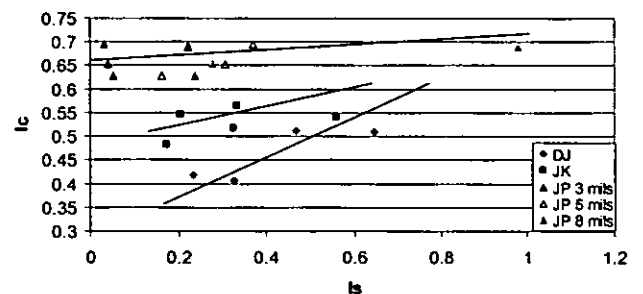


*Figure 7  Index of spalling at deflection of 5mm vs. the index of crystallinity for coatings sprayed with the DJ, JK and JP systems*

The acoustic emission characteristics during bend test are reported in Table 3.

*Table 3. Averaged Acoustic Emission Features for all coatings.*

| Sample ID | Onset of Cracking (ε%) | Event Number | Mean Energy per event (a.u.) | Cumul. Energ. (a.u.) |
|---|---|---|---|---|
| DJ2 | 0.796 | 36 | 1287 | 46338 |
| DJ4 | 1.036 | 22 | 782 | 16911 |
| DJ5 | 0.380 | 50 | 1320 | 61986 |
| DJ6 | 0.725 | 49 | 1033 | 49352 |
| JK2 | 0.291 | 99 | 620 | 60047 |
| JK4 | 0.268 | 111 | 300 | 34082 |
| JK5 | 0.180 | 87 | 673 | 58419 |
| JK7 | 0.164 | 95 | 690 | 64857 |
| JK8 | 0.451 | 172 | 239 | 40705 |
| JP1 | 0.624 | 206 | 201 | 41438 |
| JP2 | 0.555 | 65 | 714 | 45985 |
| JP3 | 0.554 | 27 | 1766 | 47869 |
| JP4 | 0.537 | 103 | 349 | 35908 |
| JP5 | 0.371 | 79 | 892 | 65933 |
| JP6 | 0.496 | 50 | 957 | 47181 |
| JP7 | 0.538 | 111 | 251 | 27804 |
| JP8 | 0.552 | 55 | 699 | 38322 |
| JP9 | 0.583 | 35 | 1823 | 62895 |
| JP10 | 0.645 | 283 | 136 | 38499 |
| JP11 | 0.647 | 75 | 606 | 44974 |
| JP12 | 0.608 | 59 | 1142 | 65260 |

In analyzing the results combined with those presented earlier, it is possible to relate some of the cracking behavior to other coating properties. Comparing the data for the JP coatings, it is clear that increasing the coating thickness reduces the number of events while increasing both the mean energy per event and total energy released during the deformation. Figure 8 shows the relationship between coating thickness and the mean acoustic energy. From the literature, it was reported that coatings exhibiting well bonded splats were reported to release higher energy during the bend test [5,6]. Therefore, the amount of strain energy stored in the coating during the bend tests is proportional to the strength of the coating. It would then be reasonable to relate the total strength of a coating to the energy relesed during its rupture. A thicker coating with increased strength can store and thus release more energy while fracturing. A thicker coating will allow the formation of longer transverse cracks liberating more energy during the rupture.
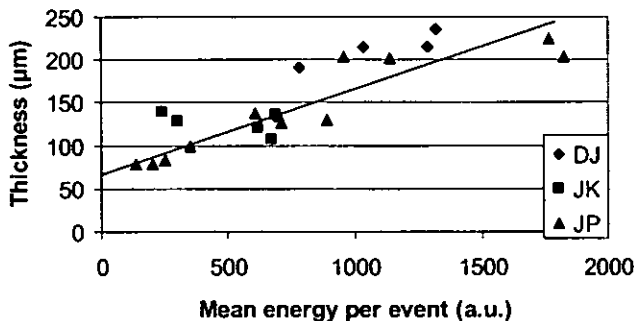
*Figure 8  Coating thickness vs. mean energy per event for samples sprayed with Diamond Jet, Jet Kote and JP-5000 guns.*

From Tables 3 and 4, it is also possible to find a general trend between the cumulative energy and the $I_s$ (Index of Spalling), indicating a larger tendency to spall for coatings releasing more acoustic energy during bending. The onset of cracking seems to be inversely related to the $I_c$ indicating that coating amorphisation delays the formation of cracks.

Figure 9 shows the relationship between the onset of cracking and the residual stress. This data is in general agreeement with empirical observations demonstrating a better resistance to crack formation associated with higher residual stresses. It should be noted that a different relationship is present for the JP-5000; this may be caused by the difference in coating crystallinity.
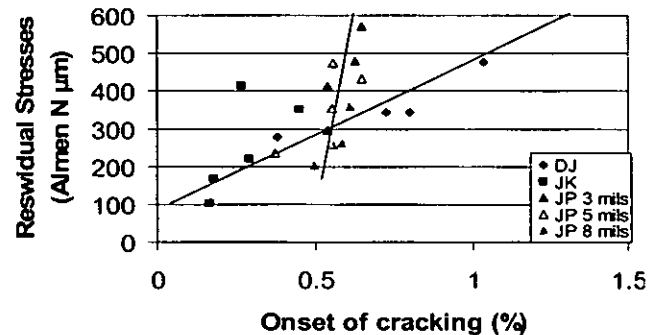
*Figure 9  Relation between onset of cracking and the residual stress for coatings sprayed with DJ, JK and JP systems.*

A tabular summary of the cyclic loading results is shown in Table 4 .

*Table 4 Cyclic loading results*

| ID | Step Loading | | | | Fatigue | |
|---|---|---|---|---|---|---|
| | Cracks | | Spalling | | Cracks | Spalling/fracture |
| | Stress (KSI) | Cycles (range) | Stress (KSI) | Cycle | Cycle (range) | Cycle (range) |
| JK2 | 180 | 40-50 | 240 | 3895 | 105(90) | 25297 (4435) |
| JK4 | 180 | 35-41 | 240 | 3210 | 4970 (9860) | 37099 (29640) |
| JK5 | 180 | 4-39 | 240 | 3673 | 75 (50) | 54703 (9454) |
| JK4 Thick | 170 | 29-61 | -- | --- | 402 (696) | 99862 (118780) |
| DJ2 | 200-210 | 51-55 | 240 | | 1950 (2900) | 12501 (454) |
| DJ4 | 230 | 39-51 | 240 | 1909 | 2100 (400) | 128902 (3666) |
| DJ5 | 190-200 | 95-19 | 240 | | 98 (55) | 12697 (2898) |
| DJ5 thick | 190 | 44-54 | - | | | 7582 (5876) |
| JP5 | 180 | 35-41 | 240 | 3810 | 38 (5) | 45028 (30156) |
| JP11 | 190 | 24-33 | 230 | 42 | 55 (10) | 12498 (585) |
| JP8 | 180 | 43-72 | 230 | | 674 (1252) | 23045 (3511) |
| JP8 Thick | 160 | 29-44 | — | | 42(7) | 2086 (4095) |

These data are presented graphically in Fig. 10 for the DJ. It can be noticed that cracking is generally occurring at lower stresses or cycles than spalling of coatings. The line in Fig. 10 presents the expected 300 fatigue life as per Mil-Handbook 5 data for a R ratio of -0.55. It is evident that even though cracking occurs at a relatively low number, no debit on the sample life was caused by either coating spalliation or sample fracture. This leads to the observation that for coatings in the range of .003-.005" thickness, a coating cracking threshold of 180 ksi and a spalling threshold of 240 ksi should be routinely expected regardless of the system being used. However,

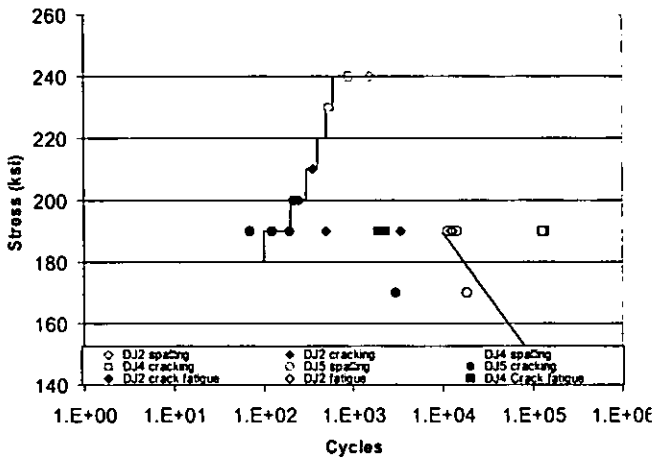unfotunately, it is very difficult to relate the formation of cracks to the occurrence of spalling.



*Figure 10  DJ Coating Integrity and Fatigue Performance*

In an attempt to develop a quality control tool assessing the performance of coating subjected to cyclic loading, it seemed more useful to relate the coating microstructure and performance in bending to the crack initiation at constant maximum load. Therefore, the fatigue results at 1310 MPa (190 ksi) were used. Figure 11 shows that by graphically depicting the results of the bend test against either the ratio of the onset of cracking/in-flight particle temperature (filled symbols) or the onset of cracking/ $I_C$ (crystallinity index), a direct and useful relationship can be established. Indeed coating with higher residual stresses processed at higher temperature would require a larger number of cycles before cracking in fatigue.
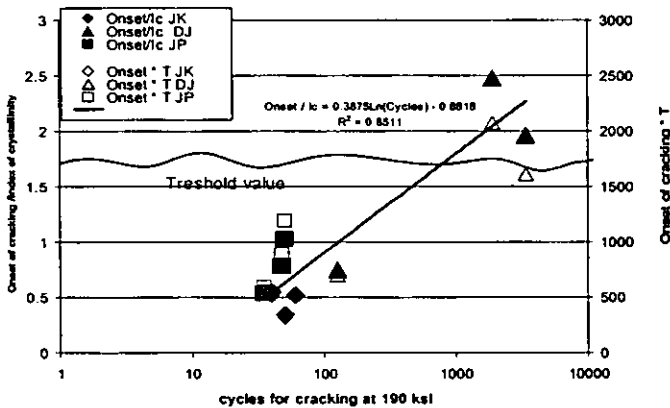


*Figure 11  Relationship between the number of cycles required to generate cracks in coating at stress level of 190 ksi and product onset\*T (right axis) or the ratio onset of cracking/Ic (left axis).*

## Summary

The current tools for QC are microstructure, microhardness, Almen, and tensile testing. From the data generated in this report, it appears that coating performance is governed by a

combination of properties including hardness, residual stress (which regulates the onset of cracking) and $I_C$ (or by the T (temperature) during processing as shown in Fig. 4. It would therefore make logical sense to consider use of temperature/velocity monitoring systems for process control. Also, in order to include some mechanical test of actual coating, the inclusion of a bend test could be mandatory. The process control might include:

- The spraying of Almen strips for bend testing and the monitoring of in-flight particles.
- An alternative could be spraying of multiple Almen strips, perform bend testing and then subsequent X-ray diffraction to measured the amount of amorphous phase ($I_c$).

From the information gathered, these methods are reliable in differentiating between varied processes from the varied gun as shown in previous sections.

A tentative conclusion can be drawn that higher processing temperatures can provide higher residual stress (expected) but this is also in conjunction with more amorphous phase or less crystallinity. Thus, the characterization indicates this residual stress/amorphous phase combination will extend the onset of cracking but the relationship with spalling tendency is still not clear given the limited data.

The bottom line conclusion: the ratio between onset of cracking and the $I_C$ (index of crystallinity)//product of onset and maximum process temperature appears to provide a threshold concerning both the cracking and fatigue cycle performance.

## Reference

1. Bouaricha, S., Marcoux, P. and Legoux, J.-G. *Bending Behaviour of HVOF Produced WC-17Co Coating Investigated by Acoustic Emission.* Journal of Thermal Spray Technology. Vol.13, No. 3, Sept. 2004, pp.405-414.
2. Bouaricha S. and J.-G. Legoux. "Strain Tolerance Characterization for HVOF Coatings Using the Acoustic Emission Tool". Published in 'Proceeding of the ITSC 2004', Osaka, Japan.
3. Dalmas D., S. Benmedakhene, C. Richard, A. Laksimi, Characterization of cracking within WC-Co coated materials by an acoustic emission method during four point bending tests, Proceeding of ITSC, Montréal 2000, pp.1335-1340.
4. Miguel J.M., J. M. Guilemany, B.G. Mellor and Y. M. Xu. Materials Science and Engineering A352 (2003) 55-63.
5. Kucuk A., C. C. Berndt, U. Senturk, R. S. Lima and C. R. C. Lima, Influence of Plasma spray parameters on mechanical properties of yttria stabilized zirconia coatings. I: Four point bend test, Materials Science and Engineering. A284, 2000, p 29-40.
6. Driver L.C., P.H. Shipway, D.G. McCartney, L.A. Donohue and D.S. Rickerby. Thermal Spray 2003: Advancing the Science & Applying the Technology, (Ed.) C. Moreau and B. Marple, Published by SM International, Materials Park, Ohio, USA, 2003, pp. 15-20.